Acta of Bioengineering and Biomechanics
Vol. 18, No. 3, 2016

Original paper
DOI: 10.5277/ABB-00476-2015-03

$sZrO_2$-CeO_2 ceramic powders obtained from a sol-gel process using acetylacetone as a chelating agent for potential application in prosthetic dentistry

DAMIAN NAKONIECZNY[1]*, ZBIGNIEW PASZENDA[1], SABINA DREWNIAK[2], TOMASZ RADKO[3], MARCIN LIS[4]

[1] Department of Biomaterials and Medical Devices Engineering, Silesian University of Technology, Zabrze, Poland.
[2] Department of Optoelectronics, Silesian University of Technology, Gliwice, Poland.
[3] Institute for Chemical Processing of Coal, Zabrze, Poland.
[4] Institute of Non-Ferrous Metals, Division of Powders and Composite Materials, Gliwice, Poland.

Purpose: The main objective of this study was to obtain single-phase β-ZrO_2 powders with so-called *soft agglomerates* reproducibile morphology with acetyl-acetone as a chelating-agent. To the best of our knowledge there is no avaiable data which determine the effect of acetyl acetone on the phase composition and morphology of ceria-doped ZrO_2 powders for biomedical applications. *Methods*: Twenty variants of powders with different water to zirconia precursor and acetylacetone to zirconia precursor molar ratios were prepared. $0.9ZrO_20.1CeO_2$ powders were obtained by a hydrolysis and condensation and further calcination of zirconium *n*-propoxide in a simple one-step sol-gel process. Influence of acetyloacetone to zirconia precursor on the phase composition ratio and water to zirconia precursor was investigated. Samples have been characterized by X-ray diffraction (XRD), Raman spectroscopy (RS), thermal analysis (TGA/DTA) and scanning electron microscopy (SEM) measurements. *Results*: Ceramic powders prepared by sol-gel process, according to the various concentration of chelating agent and water show different morphology and phase composition. *Conclusions*: Higher molar ratios of AcAc in range with smaller amounts of water cause hard agglomerates, obtained powders are characterized by highly thermally stable behaviour and various phase composition. With higher molar ratios of water to zirconium-*n*-propoxide so-called *soft agglomerates* and one phase powders are obtained.

Key words: *sol-gel process, X-ray METHODS, thermal analysis, ZrO_2, prosthetic dentistry*

1. Introduction

Zirconia is a type of advanced ceramic used as a thermal barrier coating in plane industry, anti-abrasive coating for cutting tools and as a functional ceramic in biomedical applications [5], [11]. Due to its mechanical strength and white color, it has been applied to dental restorations made by CAD/CAM [13], [19]. However, use of zirconia in dentistry raises a lot of reservations and is associated with reports of uncontrolled phase transformation from tetragonal (β) to monoclinic (α), which occurs in oral environments [3], [16]. Such a transformation results in an increase of zirconia volume and possible cracking of prostheses. This is so-called low-temperature degradation, which especially accelerates in humid environments and with elevated temperature [2], [3], [14]. It has been proved that in order to prevent the unfavorable transformation of β-ZrO_2 is doping zirconia with metal oxides, which stabilizes the tetragonal phase in a crystal lattice and ensures the nanoscale grain size [9], [10]. Currently, the most commonly used dopant is Y_2O_3, which, however, does not fully ensure stability of β phase for degradation processes in human body environment [5], [11]. Based on some research results, it can be assumed that CeO_2, as a dopant, provides complete stability of the β phase and uniform grain size [5], [18], [23]. Stabilization of β-ZrO_2 structure of cerium oxide is possible thanks to the

* Corresponding author: Damian Nakonieczny, Department of Biomaterials and Medical Devices Engineering, Silesian University of Technology, ul. Roosevelta 40, 41-800 Zabrze, Poland, Tel: +480322777451, e-mail: damian.nakonieczny@polsl.pl
Received: September 25th, 2015
Accepted for publication: December 12th, 2015

oxygen vacancies, which further stiffen the lattice network, preventing the unfavorable phase transformation [10], [15]. Another factor that makes CeO_2 a good stabilizer of the β phase is that Ce^{4+} ion has a similar atomic radius to the Zr^{4+} ion, which additionally stiffens the zirconia crystal lattice [4].

The method of preparing ceramic powders is also very important for stabilization. One of the best preparation methods available is the sol-gel process because it allows for strict control of the chemical composition and obtaining a homogeneous grain size distribution [6], [20], [23]. Therefore, the objective of this study is to prepare, using the sol-gel method, single-phase β-ZrO_2 powders doped with CeO_2 with so-called *soft agglomerates* reproducible morphology effect. The phase composition of ceramic powders is an important factor for ceramic implant resistance to low-thermal-degradation in the body fluids environment. Only homogeneous β-ZrO_2 ceramics is suitable for medical applications [9]. It is therefore essential that the phase composition was homogeneous as throughout all the production stages of biomedical ceramic from powders technology, green bodies preparations, compactions and solid ceramics. To the best of our knowledge, there is no information in the literature regarding the determination of the effect of acetyl acetone on the phase composition and morphology of ceria-doped ZrO_2 ceramic powders. We believe that the investigation being undertaken is useful and worth further development of zirconia ceramics for CAD/CAM systems.

2. Materials and methods

2.1. Sample preparation

Zirconium *n*-propoxide (ZNP) (Acros Organics), 2-propanol (PrOH) (analytical grade, Avantor), acetylacetone (AcAc) (Aldrich), cerium nitrate hexahydrate (CNH) (Sigma Aldrich) and ultrapure water were used as starting materials. All reagents were used without further purification. The whole sol-gel synthesis and reagent dosing were carried out in nitrogen in a humid-free environment. Stabilization of the zirconia precursor was achieved by the addition of acetylacetone (chelating agent). Based on previous empirical data, the molar ratio of AcAc and ZNP was fixed between 0.19 and 0.75, thus obtaining full-homogeneous sols and gelation times below 24 hours. The molar ratio of water and ZNP was varied between 2 and 10 with the ratio changing every second step. The molar ratio of PrOH and ZNP was held constant at 2:1. The molar ratios of 20 variants of colloidal systems are presented in Table 1. Composition of the final powder has been calculated at 0.9 mol% ZrO_2 and 0.1 mol% CeO_2. CNH was introduced into the sealed three neck round flask as a 1 M solution in PrOH. Due to its high reactivity, water was mixed at half volume with calculated propanol and carefully added drop-by-drop as the last reagent to the sol. Obtained gels were dried at 80 °C for 24 h and later ground with mortar and pestle. Ground powders were calcined in a 2.5 h pre-heating step and at 750 °C. Subsequently, powders were again ground in a hand mortar. The block diagram in Fig. 1 shows the stages of laboratory procedure.

Table 1. Molar ratios of prepared sols

Sample	ZNP	PrOH	H_2O	AcAc
A_1	1	2	2	0.75
A_2	1	2	4	0.75
A_3	1	2	6	0.75
A_4	1	2	8	0.75
A_5	1	2	10	0.75
A_6	1	2	2	0.58
A_7	1	2	2	0.38
A_8	1	2	2	0.19
A_9	1	2	4	0.58
A_{10}	1	2	4	0.38
A_{11}	1	2	4	0.19
A_{12}	1	2	6	0.58
A_{13}	1	2	6	0.38
A_{14}	1	2	6	0.19
A_{15}	1	2	8	0.58
A_{16}	1	2	8	0.38
A_{17}	1	2	8	0.19
A_{18}	1	2	10	0.58
A_{19}	1	2	10	0.38
A_{20}	1	2	10	0.19

2.2. Characterization

X-ray diffraction measurements were performed on a Seifers XRD7 diffractometer equipped with Co Kα radiation (λ = 0.179021 nm). The Raman spectra were taken with N-TEGRA Spectra (NT-MDT); wavelength equalled 633 nm. The TGA/DTA studies were carried out on a Q 1500D (MOM) in static air with a heating rate of 10° min^{-1} in the range from 24 to 1000 °C. The morphology and level of the agglomeration was evaluated by SEM analysis. Microphotographs were taken with FEI INSPECT S50 microscope.

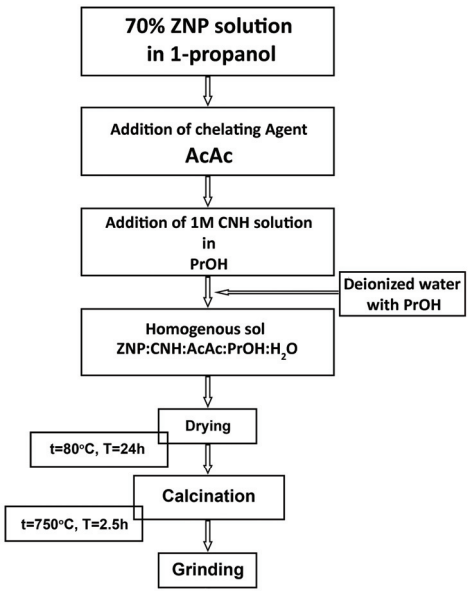

Fig. 1. Preparation procedure of $0.9ZrO_20.1CeO_2$ powders via controlled hydrolysis and condensation

3. Results

3.1. Synthesis

Powders obtained according to the molar ratios of AcAc and water showed differences in the structure, agglomeration and, in a few cases, in phase composition. Powders where the molar ratio of water was higher than that expected from the stoichiometry were characterized by a very high degree of agglomeration. This dependence is observed for all samples in the examined range from 2 to 10, as analyzed against water:ZNP. In the systems where the water ratio was significant (from 6 to 10), the solids obtained were represented as very large "cauliflower-shaped" particles, which were very easy to grind in the mortar, resulting in smaller particles. However, a greater content of AcAc with a smaller amount of water obtained large, monolithic, crystal-like agglomerates which were hard to disintegrate with a hand mortar. This situation particularly favors molar ratios of AcAc between 0.38 and 0.58 and the water from 2 to 4. Obtained powders based on their morphology were classified into two groups: soft agglomerates and hard agglomerates [17]. Comparative macroscopic images of soft and hard agglomerates powders after drying are shown in Fig. 2.

3.2. Characterization

3.2.1. Thermal studies

Figures 3a–c show the samples of thermograms for extreme molar ratios of AcAc and water; for comparison, an example of intermediate ratios is also given. From the TG curve it is clear that increasing concentration of AcAc leads to greater shrinkage after calcination. For samples with a molar ratio of AcAc:ZNP (0.75÷0.38) and the ratio of water:ZNP (2÷4), it was found that weight loss of the powders after calcination is in the range of 41.5 to 72% and corresponds to the sample shown in figure (Fig. 3a). For low molar ratios of AcAc: ZNP (0.19) and water from 6 to 10, weight loss was 30–35%, thermograms being similar as shown in Fig. 3c. Powders with an intermediate relationship of ZNP:H_2O (4 to 6) and the ZNP:AcAc (0.38÷0.58) similarly were characterized by various weight loss in the range from 37 to 48% (Fig. 3b). Depending on the molar ratios of ZNP:H_2O and ZNP:AcAc, it is possible to identify the characteristic peaks. On this basis, from the samples with significant differences in thermal behaviour, 3 powder samples A_1, A_3, and A_{14} were chosen for phase composition and morphology testing by SEM. The curves from the other samples were rejected due to the lack of repro-

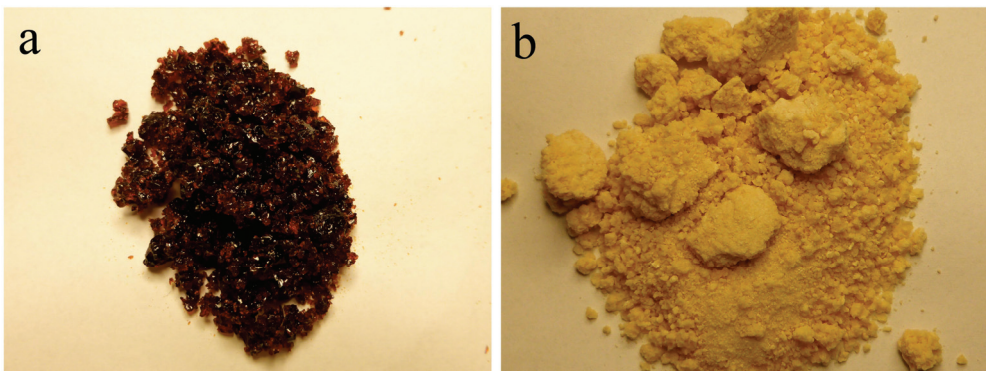

Fig. 2. Comparative photos of: (a) "hard agglomerates", (b) "soft agglomerates"

ducibility and will not be taken into account in future research.

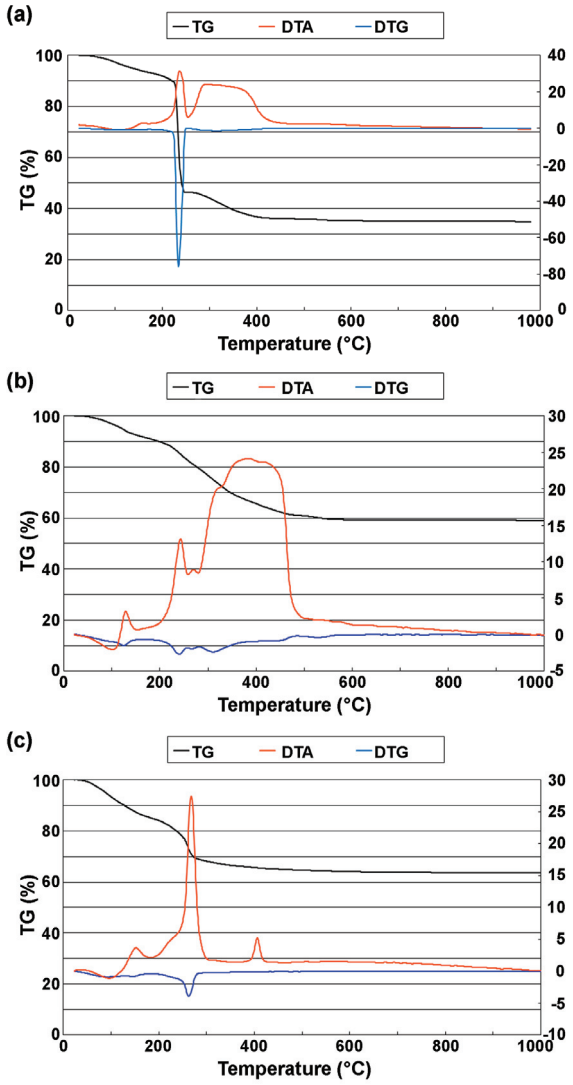

Fig. 3. Thermograms of (a) A_1), (b) A_3, (c) A_{14}

3.2.2. X-ray diffraction

The composition and the structure of A_1, A_3, and A_{14} were confirmed by XRD analysis. Figure 4a and b exhibits the examples of diffraction plots of the two most differentiated powder samples: A_3 and A_{14}. The XRD pattern of A_1 was similar to A_{14} with a slightly less intensity peaks. For A_3 we found a pure monoclinic phase, the peaks at 2θ = 28.49°, 32.88°, 36.70°, 40.21°, 47.71°, 52.53°, 58.95°, 59.53°, 65.31°, 78.04°. For the pure regular phase, the peaks at 2θ = 35.55°, 59.60°, 71.56°. Sample (b) is full tetragonal as is A_1. For the pure tetragonal phase, peaks were 2θ = 34.99°, 40.27°, 40.80°, 58.64°, 59.07°, 69.80°, 70.54°, 73.92°. A full description of the XRD-peaks is given in Table 2.

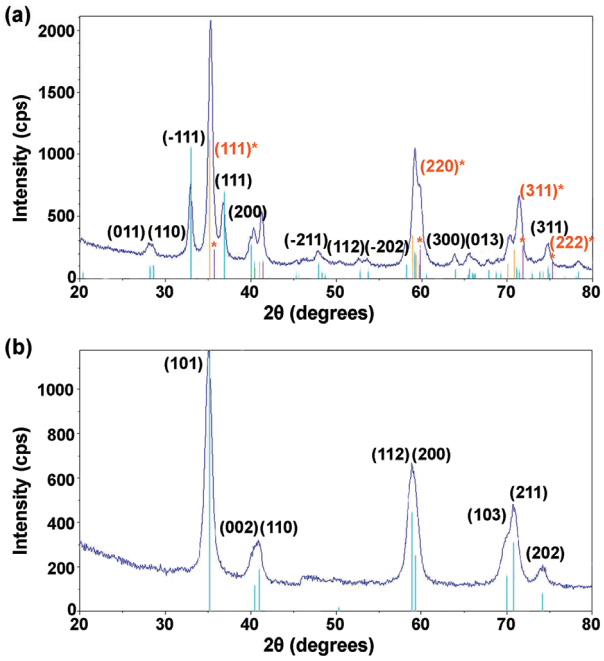

Fig. 4. XRD patterns of: (a) A_3, (b) A_{14}
*cubic phase

Table 2. Full description of X-ray patterns from Fig. 4

A_3		
2θ(degrees)	hkl	Phase
20.279	100	Monoclinic
28.019	011	
28.484	110	
32.882	–111	
36.969	111	
41.230	200	
47.712	–211	
48.128	102	
52.526	112	
53.455	–202	
58.948	220	
63.671	300	
65.314	013	
65.630	–113	
67.546	–311	
68.454	–131	
71.121	–302	
74.453	311	
78.036	222	
35.551	111	Cubic
59.596	220	
71.556	311	
74.963	222	
A_{14}		
34.99	101	Tetragonal
40.269	002	
40.800	110	
50.096	102	
58.664	112	
59.069	200	
70.535	211	
73.915	202	

3.2.3. Raman spectroscopy

The obtained phase compositions were additionally confirmed by Raman spectroscopy. Figure 5 a–b displays the Raman spectra for samples A_3 and A_{14}. Five bands at 147, 268, 313, 460, and 600 cm^{-1} correspond to the Raman-active modes, which correspond to the β-ZrO_2 phase ($1A_g+2B_g+3E_g$; Fig. 5a.) [22].

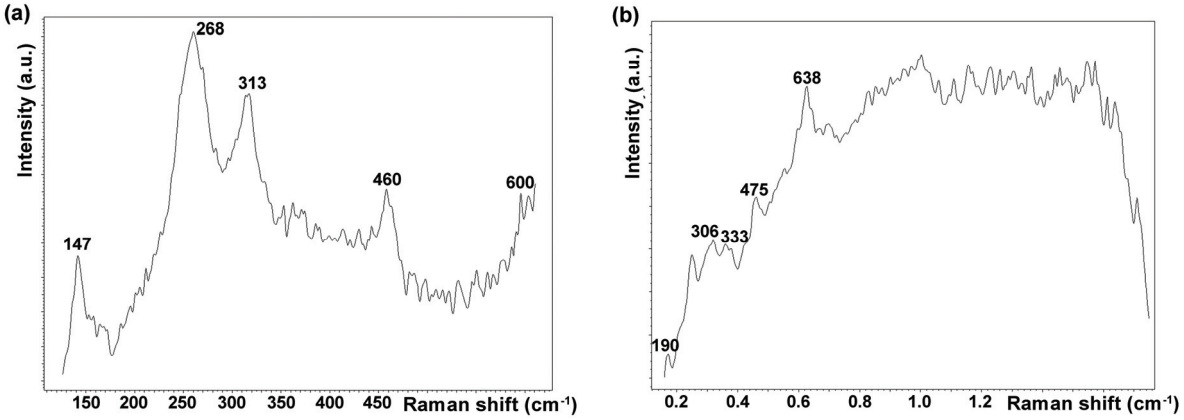

Fig. 5. Raman spectra for: (a) A_{14} – full tetragonal ceria-doped zirconia, (b) A_3 – monoclinic-tetragonal ceria-doped zirconia

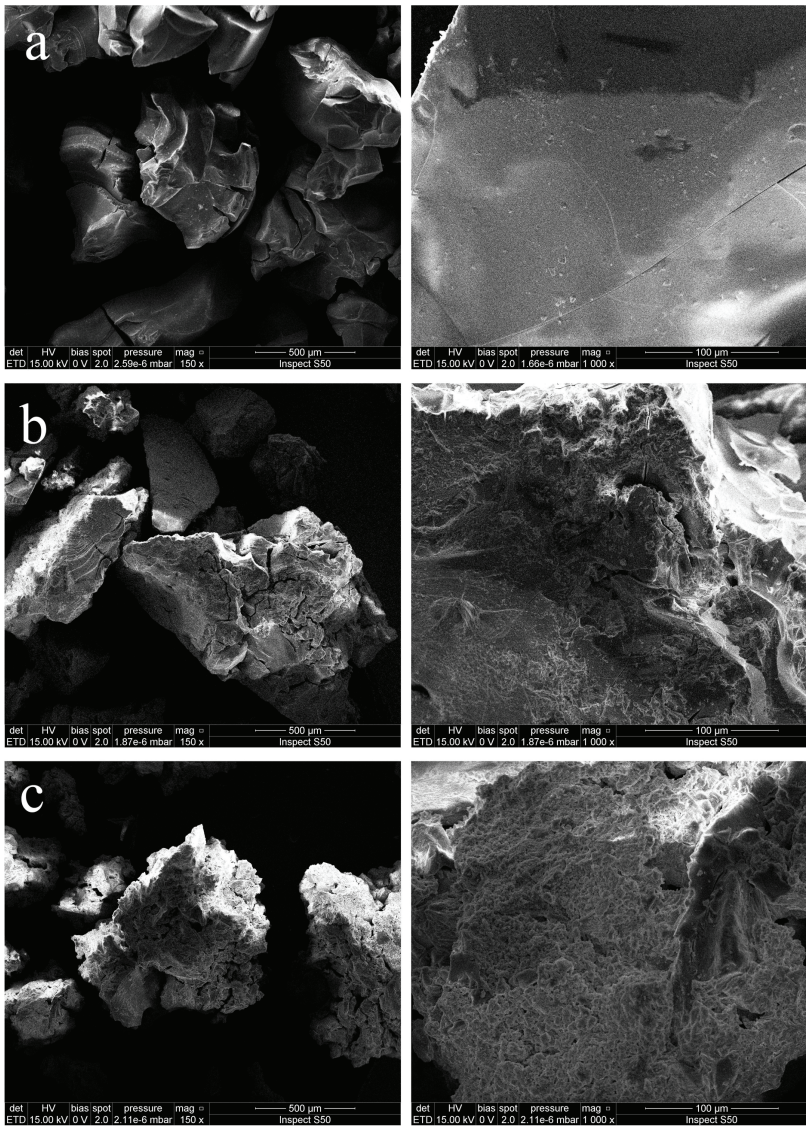

Fig. 6. SEM images of the as-obtained powders: (a) A_1, (b) A_{11}, (c) A_{17}

Monoclinic zirconia is seen in spectrum bands at 190, 306, 333, 475, and 638 cm^{-1} (Fig. 5b) [7]. In addition, there was observed the presence of cubic fluorite CeO_2 band at 465 cm^{-1}, which is a clear sign of inhomogeneity in this powder variant.

3.2.4. Morphology studies

Figure 6a–c shows SEM microphotographs of samples A_1, A_{11} and A_{17}. Based on the SEM images, the difference between prepared powders with changing molar ratios of the ZNP:AcAc:H_2O can be clearly seen. In Fig. 6a, big, solid sharp-edged grains in the size range 250–500 μm are clearly seen. Additionally, there is a very low degree of grain agglomeration. Figure 6c shows sample A_{17} with radically different morphology. The A_{17} grains are significantly smaller, characterized by a considerable degree of agglomeration. From the appearance of breakthrough at the edge it can be stated that they are much softer than those from sample A_1. An intermediate situation is observed for sample A_{11} (Fig. 6b).

4. Discussion

4.1. Synthesis

The well-known parameters of the sol-gel process strongly influenced the properties of the gel and final powders and especially the subsequent thermal evolution [17]. Caruso et al. [17] reported the occurrence of so-called *soft* and *hard-agglomerates*, whose shape corresponds with those obtained in our work. The binding mechanism of soft-agglomerates corresponds to the formation of weak bonds of close-range van der Waals forces, and, therefore, the resulting powders can be easily disintegrated. On the other hand, hard agglomerates are held together by strong binding forces (chemical bonds in solid bridges) [17]. The shape and morphology of the powders obtained are very important for the preparation of green bodies and subsequent sintering of the CAD/CAM blocks. Powders from hard agglomerates require a higher pressing pressure; their structure favors inhomogeneity and the appearance of pores in green bodies. This requires raising the temperature and time of sintering, which leads to adverse changes in the phase composition of zirconia. The powders from soft-agglomerates improve sinterability, high packing density and good flowability [17].

4.2. Characterization

4.2.1. Thermal studies

For samples A_1, A_2, A_6, and A_9, TGA curves were similar (Fig. 3a.). Thermal decomposition was almost explosive, as can be seen from a high endothermic peak at about 233 °C, associated with the rapid decomposition of propanol, whose temeperature of decomposition was shifted due to the formation of a very stable complex between zirconia propoxide and AcAc. The big exotermic broad bump occurring in the range 248–431 °C is associated with the thermal decomposition of AcAc [12], [21]. In contrast, a very small endothermic peak in the range from 82 to 134 °C is associated with the evaporation of water.

TGA curves presented in Fig. 3b correspond to the curves of samples A_3, A_4 and A_5. The presence of four characteristic peaks can be identified on the curves: endothermic 60–110 °C, associated with the evaporation of water; exothermic at approximately 135 °C, associated with the disintegration of propanol; exothermic at 242 °C, associated with decomposition of AcAc; and a big broad exothermic bump between 267–490 °C, which we expected came from crystallization of a new phase.

The curves in Fig. 3c were characteristic of powders A_{11}, A_{13}, A_{14}, A_{17}, A_{19} and A_{20}. We have identified four characteristic peaks: endothermic associated with the evaporation of water at 60–110 °C; exothermic at 140 °C, associated with the disintegration of propanol; exothermic at 265 °C, associated with the disintegration of AcAc; and a small sharp exothermic peak at 400 °C that probably came from the crystallization of another new phase but different than it was in the case of curves shown in Fig. 3c.

4.2.2. Phase composition (XRD and Raman spectra)

Based on the results of XRD, we verified the presence of characteristic “new-phase” peaks in the TGA of curves. The presence of a broad exothermic bump in the A_3 sample between 267–490 °C corresponds to the monoclinic phase (α-ZrO_2) crystallization. For A_{14} there occurs a small sharp exothermic peak at 400 °C that corresponds with the crystallization of zirconia tetragonal phase (β-ZrO_2), which seems to confirm the result of XRD patterns. Referring this result to the ZNP:H_2O:AcAc molar ratios, we saw that the crystallization of the β-ZrO_2 phase favors the ratios of ZNP:AcAc in the range of 0.19–0.38 and the ZNP:H_2O in

the range from 6 to 10. In contrast, crystallization of the α phase has a favorable ratio of ZNP:AcAc is equal to 0.75 and the ZNP:H_2O from 6 to 10. Interestingly, sample A_1 has a high molar ratio of AcAc (0.75) and thus increasing the thermal stability does not cause any crystallization of α-ZrO_2 phase. Based on the data in Table 1, it can be stated that this situation is the result of a lower ratio of ZNP:H_2O. Also, there are no TGA curves, even at the same *new phase* peak as in the A_{14} curve, which may be explained by the "camouflage" by decomposing AcAc at a temperature range from 248 to 431 °C – exactly as in the crystallization temperature zone of β-ZrO_2 at 400 °C. The use of Raman spectroscopy allowed the results obtained by X-ray techniques to be confirmed.

4.2.3. Morphology studies

Comparing morphology of the powders to the molar ratios, it is clear that the high ratio of ZNP:AcAc (0.75) with low water contents promotes the same formation as described by Caruso et al. [19], the so-called *hard agglomerates*. However, increasing the ratio of ZNP:H_2O over 4 and decreasing the ratio of ZNP:AcAc below 0.38 resulted in the presence of *soft agglomerates*, which makes it possible to obtain full-value ceria-doped zirconia solid green bodies. [17].

5. Conclusion

1. This work described the influence of molar ratios of chelating agent and water on a zirconia precursor as observed in phase composition and macroscopic morphology of $0.9ZrO_20.1CeO_2$ powders. It was expected that a molar ratio of AcAc and water to ZNP plays an important role in agglomerate morphology, phase composition and thermal behavior during calcination.
2. According to the data obtained, it can be stated that higher molar ratios of AcAc in the range 0.58–0.75 with smaller amounts of water (2÷4) cause hard agglomerates, highly thermally stable powders with various phase composition.
3. Water molar ratios higher than 6 and AcAc ratios that are reduced below 0.38 predispose obtaining so-called *soft agglomerates* and powders with full tetragonal structure. This is particularly desirable for CAD/CAM prothetic system blocks manufacturing.
4. We hope that the obtained results will allow us, in our future studies, to prepare zirconia-ceria green bodies and produce valuable blocks for CAD/CAM systems with suitable properties like poor porosity, very good compressibility and exceptionally stable mechanical properties in oral environments.

References

[1] BERENDTS S., LERCH M., *Growth and characterization of low yttria-doped fully cubic stabilized zirconia-based single crystals*, J. Cryst. Growth, 2013, Vol. 371, 28–33.

[2] BORCHERS L., STIESCH M., BACH F.W., BUHL J.-CH., HÜBSCH CH., KELLNER T., KOHORST P., JENDRAS M., *Influence of hydrothermal and mechanical conditions on the strength of zirconia*, Acta Biomater., 2010, Vol. 8, 4547–4552.

[3] CATTANI-LORENTE M., SCHERRER S.S., AMMANN P., JOBIN M., WISKOTT H.W.A., *Low temperature degradation of a Y-TZP dental ceramic*, Acta Biomater., 2011, Vol. 7, 858–865.

[4] CHAIM R., BASAT G., KATS-DEMYANETS A., *Effect of additives on grain growth during sintering of nanocrystalline zirconia alloys*, Mater Lett., 1998, Vol. 35, 245–250.

[5] CHEVALIER J., GREMILLARD L., VIKAR A.V., CLARKE D.R., *The Tetragonal – Monoclinic Transformation in Zirconia: Lessons Learned and Future Trends*, J. Am. Ceram. Soc., 2009, Vol. 92(9), 1901–1920.

[6] COLOMER M.T., *Straightforward synthesis of Ti-doped YSZ gels by chemical modification of the precursors alkoxides*, J. Sol-Gel. Sci. Technol., 2013, Vol. 67, 135–144.

[7] COURTIN E., BOY P., PIQUERO T., VULLIET J., POIROT N., LABERTY-ROBERT C.A., *Composite sol-gel process to prepare a YSZ electrolyte for Solid Oxide Fuel Cells*, J. Power Sour., 2012, Vol. 206, 77–83.

[8] DEL MONTE F., LARSEN W., MACKENZIE J.D., *Stabilization of tetragonal ZrO_2 in ZrO_2-SiO_2 binary oxides*, J. Am. Ceram. Soc., 2000, Vol. 83(3), 628–634.

[9] EN ISO 13356:2013, Implants for surgery. Ceramic materials based on yttria-stabilized tetragonal zirconia (Y-TZP).

[10] FÁBREGAS O., FUENTES R.O., LAMAS D.G., FERNÁNDEZ DE RAPP M.E., DE RECA N.W., FANTINI M.C.A., CRAIEVICH A.F., PRADO A.F., MILLEN R.P., TEMPERINI M.L.A., *Local structure of metal-oxygen bond in compositionally homogeneous, nanocrystalline zirconia-ceria solid solutions synthesized by a gel-combustion process*, J. Phys. Condens Matter., 2006, Vol. 18, 7863–7881.

[11] HANNINK R.H.J. KELLY P.M., MUDDLE B.C., *Transformation toughening in zirconia ceramics*, J. Am. Ceram. Soc., 2000, Vol. 83(3), 461–487.

[12] HUANG W., YANG J., WANG CH., ZOU B., MENG X., WANG Y., CAO X., WANG Z., *Effects of Zr/Ce molar ratio and water content on thermal stability and structure of ZrO_2-CeO_2 mixed oxide prepared via sol-gel process*, Mater Res. Bull., 2012, Vol. 47, 2349–2356.

[13] KELLY J.R., DENRY I., *Stabilized zirconia as a structural ceramic: An overview*, Dent. Mater., 2008, Vol. 24, 289–298.

[14] KEUPER M., BERTHOLD CH., NICKEL K.G., *Long-time aging 3 mol.% yttria-stabilized tetragonal zirconia polycrystals at human body temperature*, Acta Biomater., 2014, Vol. 10, 951–959.

[15] LEBRUN N., PERROT P., *Cerium-Oxygen-Zirconium*, [in:] *Refractory metal systems: phase diagrams, crystallographic*

and thermodynamic data, Materials Science International Services GmbH, Stuttgart, 2010, 87–110.

[16] LUGHI Y., SERGO V., *Low temperature degradation-aging-of zirconia: A critical review of the relevant aspects in dentistry*, Dent. Mater., 2010, Vol. 26, 807–820.

[17] MAMANA N., DÍAZ-PARRALEJO A., ORTIZ A.L., SÁNCHEZ-BAJO F., CARUSO R., *Influence of synthesis process on the features of Y_2O_3-stabilized ZrO_2 powders obtained by the sol-gel method*, Ceram. Int., 2014, Vol. 40, 6421–6426.

[18] MENVIE BEKALE V., LEGROS HAUT C., SATTONNAY G., HUNTZ A.M., *Processing and microstructure characterization of ceria-doped yttria-stabilized zirconia powder and ceramics*, Solid State Ionics, 2006, Vol. 177, 3339–3347.

[19] MIYAZAKI T., HOTTA Y., *CAD/CAM systems available for the fabrication of crown and bridge restorations*, Aust. Dent. J., 2011, Vol. 56(1), 97–106.

[20] NAKONIECZNY D., WALKE W., MAJEWSKA J., PASZENDA Z., *Characterization of magnesia-doped yttria-stabilized zirconia powders for dental technology applications*, Acta Bioeng. Biomech., 2014, Vol. 13(4), 99–106.

[21] NAUMENKO A., GNATIUK I., SMIRNOVA N., EREMENKO A., *Characterization of sol-gel derived TiO_2/ZrO_2 films and powders by Raman spectroscopy*, T. Sol Films, 2012, Vol. 520, 4541–4546.

[22] NAVIO J.A., MARCHENA F.J., MACIAS M., SANCHEZ-SOTO P.J., PICHAT P., *Formation of zirconium titanate powder from a sol gel prepared reactive precursor*, J. Mater Sci., 1992, Vol. 27, 2463–2467.

[23] TRUSOVA E.A., KHRUSHCHEVA A.A., VOKHMINTCEC K.V., *Sol-gel synthesis and phase composition of ultrafine ceria-doped zirconia powders for functional ceramics*, J. Eur. Ceram. Soc., 2012, Vol. 32, 1977–1981.